Virchows Arch (2000) 436:147–157 

ORIGINAL ARTICLE

**Steffen Sandmann · Rainer M. Bohle**
**Thomas Dreyer · Thomas Unger**

# The T-type calcium channel blocker mibefradil reduced interstitial and perivascular fibrosis and improved hemodynamic parameters in myocardial infarction-induced cardiac failure in rats

Received: 16 March 1999 / Accepted: 23 August 1999

**Abstract** Fibrillar collagen accumulates within the interstitium and around coronary arteries following cardiac failure and is responsible for abnormal myocardial stiffness and reduced coronary performance associated with impaired cardiac function. The aim of the study was to determine the effects of long-term treatment with the T-type calcium channel antagonist mibefradil on myocardial remodeling and cardiac function after chronic myocardial infarction (MI). MI was induced by permanent ligation of the left coronary artery in male Wistar rats. Animals were assigned to sham-operated, placebo-treated or mibefradil-treated (10 mg/kg per day p.o.) MI groups. Treatment with mibefradil was started either 7 days before, 24 h after, or 7 days after ligation and continued for 6 weeks after MI. At this time point, mean arterial blood pressure (MAP), heart rate (HR), left ventricular end-diastolic pressure (LVEDP) and cardiac contractility ($dP/dt_{max}$) were measured in conscious rats. Morphometric parameters were determined in picrosirius red-stained hearts: total heart weight (THW), interstitial and perivascular collagen volume fraction (ICVF, PCVF), myocardial infarct size (IS), vascular perimeter (VP), inner vascular diameter (IVD) and media thickness (MT). Six weeks after MI, MAP and $dP/dt_{max}$ were decreased, and LVEDP was increased in placebo-treated animals. In mibefradil-treated animals whose treatment started 7 days before or 24 h after MI, MAP and $dP/dt_{max}$ were higher, and LVEDP was lower than in placebo-treated controls. THW, ICVF, PCVF and MT were higher in placebo-treated animals. Mibefradil treatment resulted in higher ICVF and IS, higher VP and IVD (when started 7 days before MI) and lower PCVF and MT (when started 7 days before or 24 h after MI) than were observed in placebo-treated controls. Chronic treatment with mibefradil reduced interstitial and perivascular fibrosis and improved cardiac function in MI-induced heart failure in rats. Cardiac remodeling was best prevented when treatment was begun before the ischemic event.

**Key words** T-type calcium channel blockade · Mibefradil · Myocardial infarction · Cardiac remodeling · Rat

S. Sandmann (✉) · T. Unger
Institute of Pharmacology,
Christian-Albrechts-University of Kiel,
Hospitalstrasse 4, D-24105 Kiel, Germany
e-mail: s.sandmann@pharmakologie.uni-kiel.de
Tel.: +49-431-5973503
Fax: +49-431-5973522

R.M. Bohle · T. Dreyer
Institute of Pathology,
Justus-Liebig-University of Giessen, Giessen, Germany

## Introduction

The myocardium contains muscle fibers, blood vessels and a connective tissue skeleton. The myocardial collagen matrix and the highly organized collagen network are the structural continuum of this connective tissue, serving the maintenance of architecture and mechanical function of the myocardial wall. The fibrillar type I and III collagens are the major components of the cardiac interstitium [28, 55] which are synthesized by fibroblasts. Type I collagen is usually present in the form of thick fibers with tensile strength [9]. Therefore, the amount, composition, and distribution of this collagen type determines the tissue stiffness of the myocardium, whereas type III collagen forms fine reticular networks and is more distensible than type I collagen [14].

The development of myocardial fibrosis is related to the hypertrophic process induced by hypertension or heart failure and is characterized by an accumulation of collagen type I and III within the interstitial space and the adventitia of intramyocardial coronary arteries [49]. This process, appearing only in the absence of myocyte necrosis, is termed interstitial and perivascular fibrosis (reactive fibrosis). Later fibrosis is accompanied by scar formation after myocyte death (reparative fibrosis) [48]. During the process of reactive fibrosis, fibrillar collagen accumulates initially around coronary arteries and later

begins to radiate outward into neighboring intermuscular spaces. During the development of perivascular fibrosis, an increase in wall thickness of coronary arteries and arterioles has been shown [6]. This vascular hypertrophy seems to be responsible for the decrease in coronary vascular reserve observed in hypertension [56]. Reparative fibrosis takes place secondary to myocyte necrosis. The overall collagen volume fraction is increased more then six-fold, resulting from an enhanced collagen synthesis within existing fibroblasts and an increased fibroblast growth and proliferation [32].

While several reports have shown an increase in interstitial collagen in experimentally induced pressure overload cardiac hypertrophy [12, 14], less is known about changes in interstitial and perivascular collagen after myocardial infarction (MI). MI induces alterations in the structure of the infarcted region (scar formation) and of the noninfarcted zone (compensatory reactive hypertrophy) of the left ventricle [22] as well as of the intramyocardial vasculature [43]. This process is referred to as cardiac remodeling and describes a series of pathomorphological changes, including infarct expansion and dilatation of the noninfarcted myocardium in addition to the rearrangement of the extracellular matrix architecture, leading to cardiac hypertrophy and heart failure [1, 2]. The collagen accumulation and the consequent remodeling of the myocardium in the time after MI increase myocardial stiffness, resulting in diastolic and, ultimately, systolic ventricular dysfunction [21, 54].

Calcium channel antagonists (CCA), potent vasodilators widely used in the treatment of hypertension and angina pectoris, have been shown to prevent cardiac events after MI, to increase coronary blood flow, to attenuate myocardial fibrosis and to prevent cardiac remodeling [35, 40]. This beneficial effect of CCA has previously been attributed to their inhibiting action on the slow $Ca^{2+}$-inward current through L-type $Ca^{2+}$ channels associated with a sustained reduction of intracellular $Ca^{2+}$ accumulation in myocardial cells after cardiac injury. This inhibition of an extensive rise in cytosolic $Ca^{2+}$ by CCA is thought to reduce the activation of $Ca^{2+}$-dependent proteases and phospholipases and to prevent the production of oxyradicals [35], which are known to have the capacity to damage cardiac myocytes irreversibly and to contribute to fibrotic processes.

Mibefradil is a tetrazolium CCA featuring an inhibition of both the L- and T-type $Ca^{2+}$ channels, with a higher selectivity for T-type $Ca^{2+}$ channels [30]. The compound is a potent peripheral and coronary vasodilator and an antianginal drug [11, 41, 42]. The present study in rats was performed to determine whether long-term treatment with mibefradil affects the structural remodeling process of the heart following MI associated with functional consequences on cardiac performance. The effects of mibefradil on interstitial and perivascular myocardial fibrosis, on the structure of coronary arteries and on hemodynamic parameters were determined with reference to the start of therapy in order to establish a "therapeutic window" for any possible antifibrotic action of the drug.

## Materials and methods

Male, normotensive Wistar rats (Charles River Viga, Sulzfeld, Germany) initially weighing 230–270 g were used in the study. All experiments were performed in accordance with the German law on animal protection as released in its new version in 1993. The animals were housed individually with controlled temperature and humidity under a 12-h light/dark cycle. Rats had free access to a standard diet (Altromin: Altromin, Lage-Lippe, Germany) and to drinking water. They were divided randomly into five groups: sham operation, control MI and placebo treatment, and groups subjected to mibefradil treatment (10 mg/kg per day p.o.), with the start of treatment at different time points before and after MI as indicated below:

Group 1: Sham (sham surgery, without treatment, $n$=15)
Group 2: Placebo-treated MI (control MI, $n$=15)
Group 3: Mibafradil treatment from 7 days before MI induction ($n$=13)
Group 4: MI induced and mibafradil treatment started 24 h after ($n$=14)
Group 5: MI induced and mibafradil treatment started 7 days after ($n$=13)

After 1 week in single cages, rats in group 1 underwent a sham operation. In the rest of the animals, MI was induced by permanent ligation of the left coronary artery. Food and water intake and also body weight (BW) were measured every 2nd day before the induction of MI, every day in the first week after MI, every 2nd day in the 2nd and 3rd weeks and every 3rd day in the 4th, 5th and 6th weeks after MI, so that the drug dose could be adjusted to the individual BW. Treatment was given once daily via gastric gavage and was continued for 6 weeks after MI. Six weeks after sham operation or MI surgery arterial and venous catheters were implanted, as was a catheter in the left ventricle, to measure hemodynamic data. Hemodynamic studies were performed 24 h later in conscious rats. At the end of the experiments, 6 weeks after MI or sham operation the rats were sacrificed and the hearts were excised and fixed with 10% paraformaldehyde for morphometric studies.

### Surgical procedures

MI was induced by permanent ligation of the left coronary artery. Briefly, rats were anesthetized with ether to cannulate the tail vein for intravenous injections of methohexital sodium (10 mg/kg). The chest of each animal was shaved and disinfected. Rats were intubated and artificially ventilated with room air (50 inhalations/min, 200 $mmH_2O$, 1.5 ml/inhalation). The electrocardiogram was monitored continuously during surgery. A left thoracotomy was started by incising the skin 2 cm parallel to the third and fourth ribs. The pectoral muscles were dislocated to expose the ribs, and the incision was made at the fourth intercostal space to insert a rib-spreading chest retractor. After anterior pericardectomy the heart was exposed. The left coronary artery was then ligated intrathoracally using sterile 6-0 suture material (Ethibond, Ethicon, Norderstedt, Germany) under a stereo microscope. Successful ligation of the coronary artery was verified by the occurrence of arrhythmias in the electrocardiogram and, visually, by observation of the color changes in the ischemic area. In rats that underwent sham surgery, the ligature was placed beside the coronary artery. The thoracic cavity was closed during respiration hold. At the end of the operation procedure analgesia was induced by a subcutaneous injection of buprenorphine·HCl (0.2 mg/kg).

### Arterial, venous and left ventricular catheters

At the end of the study, 6 weeks after MI, the animals were anesthetized with ether. Anesthesia was continued by intravenous injection of methohexital sodium (10 mg/kg). Then, polypropylene

tubes (Portex, London, UK) were inserted into the right femoral artery and vein and exteriorized at the nape of the neck. The left ventricle was then cannulated using a specially constructed pig-tail catheter consisting of a PP10 tube 60 mm in length welded to a 350-mm length of PP50 tube [51]. The pig-tail at the end of the PP10 portion was inserted into the right carotid artery and advanced into the LV via the ascending aorta. During cannulation the catheter was connected to a transducer and blood pressure monitor to verify the position of the tip of the catheter. The LV was considered to be reached when the pulse pressure had a typical left ventricular configuration. The PP50 portion was then tunneled under the skin and anchored at the posterior neck region.

## Hemodynamic measurements

In preliminary experiments, the femoral artery was cannulated to measure mean arterial blood pressure (MAP) and heart rate (HR) during surgery and during the 48-h time interval after induction of MI or sham operation to determine the effect of different mibefradil dosages on peripheral hemodynamic parameters.

At the end of the study, 6 weeks after induction of MI hemodynamic measurements were performed 24 h after the implantation of the catheters in conscious rats. The femoral artery and left ventricular catheters were connected to the pressure transducers (DTX/Plus, Spectramed, Oxnard, Calif.). MAP, HR and left ventricular pressure (LVP) were obtained using two pressure processors (Gould, Valley View, Ohio). The output signals were recorded on a pen recorder (Gould Series 2000, Gould) and analyzed by a computer-based system MEGA [50] at a rate of 800 Hz. The computer program calculated the left ventricular end-diastolic pressure (LVEDP) and the maximum positive change in the left ventricular pressure signal ($dP/dt_{max}$) (1000 mmHg/s). The last parameter was considered as a marker of the myocardial contractility. Since the electrocardiogram not recorded in this part of study, LVEDP was measured at the point where the slope of the ventricular pressure signal changed from the slowly to the rapidly increasing portion [52]. This point has been shown to be closely linked to the R-wave of the electrocardiogram and to represent LVEDP in rats [51].

Rats were given time to acclimatize to the recording procedures for 30 min before baseline measurements of MAP, HR and LVP were recorded. The animals then received an intravenous infusion of the $\alpha_{a1}$-adrenoceptor agonist, methoxamine (MEX; 2.0 mg/kg per h) to increase cardiac afterload. The rate of infusion was increased steadily until MAP was elevated by about 20 mmHg. An infusion rate of 0.5–1.0 mg/h was usually necessary to attain the desired constant pressure response. This infusion rate was maintained, and a second recording was obtained. LVEDP and $dP/dt_{max}$ were calculated offline from the LVP signal using the MEGA program. MAP, HR, LVEDP and $dP/dt_{max}$ under basal conditions and during increased afterload were averaged over 5 min periods to be used in the statistical analysis.

## Tissue processing

After hemodynamic measurements, rats were sacrificed and the hearts were stored in 4% phosphate-buffered formalin in 0.15 M NaCl for morphometric examinations. After removal of the atria and large vessels, the ventricles were cut in a standardized fashion into five transversal slices from the apex to the basis using a special Plexiglas box adapted to rat hearts, which contains slits 3 mm apart for a microtome knife. Slice 5 represented the apex and slice 1, which varied in size, the basis (Fig. 1). The five slices obtained were weighed separately after the removal of clotted blood from the ventricles. The weight of all five slices was summated to obtain the total heart weight (THW), which was referred to BW (THW/BW). The slices were then transferred into 10% phosphate-buffered formalin, kept overnight, and subsequently dehydrated and embedded in paraffin by routine histological procedures. Serial 4-µm sections of each slice were cut and stained with the collagen-specific stain picrosirius red, respectively. This stain enhances

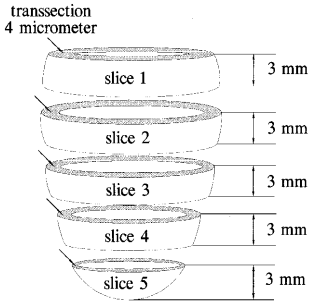


**Fig. 1** Representation of the post-mortem procedure for processing of the rat heart. Slices 1 (basis) to 5 (apex) and the position where the serial 4-µm sections of each slice were cut for staining with the collagen-specific stain picrosirius red

the natural existence of collagen fibrils, providing the means of analyzing fiber structure with greater resolution [23].

## Picrosirius red staining

The paraffin-embedded tissue sections of the five heart slices were routinely processed using a modified picrosirius red (Sirius Red, C.I. 3570, Polysciences, Warrington Pa., in aqueous picric acid) staining method described by Junqueira et al. [23]. Briefly, after being deparaffinated (2×5 min in xylol, 2×5 min in 100% ethanol, 2×5 min in 70% ethanol, 2×5 min in 50% ethanol) the 4-µm sections were washed in tap water for 10 min and in distilled water for 5 min. Then, the slices were treated for 5 min with 0.2% phosphomolybdic acid in distilled water to reduce the background. Subsequently, the 0.1% picrosirius red solution in saturated picric acid was applied for 90 min. Before dehydration (45 s in 70% ethanol, 2×3 min in 100% ethanol, 2×3 min in xylol), the slices were treated for 2 min with 0.01 N HCl and coverslipped. The interstitial and perivascular collagen regions were clearly detectable within the collagen accumulating tissue, showing a red color while the remaining tissue was yellow.

## Morphometric examinations

The morphometric parameters measured were the interstitial collagen volume fraction (ICVF) of the right ventricle and of the epicardial and the left ventricular (LV) endocardial myocardium of the septum, the perivascular collagen volume fraction (PCVF) and myocardial infarct size (IS). Vascular morphometry was investigated by determination of media thickness (MT), vascular perimeter (VP) and inner vascular diameter (IVD) of intramyocardial coronary arteries of both ventricles. Macroscopically, MI was found to be transmural in all infarcted rats. For measurement of interstitial and perivascular collagen volume fraction and of morphometric parameters of intramyocardial vessels, a computerized surface determination method with on-screen visualization of the cardiac sections (VIDAS 21, including morphometry software connected to a Leica video camera, Kontron Electronics, Eiching, Germany) was used. Sections of all five slices of the heart were placed in a universal microscope (Axioplan, Zeiss, Oberhochen, Germany). Based on the density of the picrosirius red-stained collagen fibers of tissue areas in direct light, the images were scanned systematically and computerized according to standard stereological principles described previously [46]. Accordingly, after calibration of the computerized surface determination method, the software digitized picrosirius red stained areas as white, whereas the remaining myocardium appeared in black. Owing to the homogeneous composition of the myocardial structure, these measurements were performed in eight fields (each visual field was 300 $\mu m^2$) of the right ventricle, in eight fields of the subepicardium and in eight fields of the LV endocardium of the septum for each section. ICVF was cal-

culated as the sum of all connective tissue areas divided by the sum of all connective tissue and muscle areas in the visual field of the section. Values were each averaged per measured tissue area of the section. Perivascular and infarcted areas were excluded from the measurement of ICVF. The results predict the proportion of myocardium occupied by fibrillar collagen. As previously reported, total collagen volume fraction determined by this morphometric approach is closely related to the hydroxyproline concentration of the collagen and can be used for determinations of interstitial collagen content of the heart [7, 55]. An average value for interstitial fibrosis of all five slices was used for an exact determination of the amount of cardiac fibrosis in the entire heart.

PCVF and vascular morphometry were determined from all intramural coronary arteries found in both ventricles of each section. The areas of picrosirius red-stained fields of perivascular collagen were measured by the computer program and normalized to vessel luminal area according to the method described earlier [20, 33]. Perivascular fibrosis and morphometrical parameters of coronary arteries were determined in intramyocardial vessels that had a mathematical form factor of F>0.75 (F=1 for a circle), which was calculated by the computer according to the following formula [37]:

$$F = (4\pi \times \text{vessel luminal area}) / (\text{vessel perimeter})^2$$

Average medial wall thickness of intramyocardial coronary arteries was calculated according to the recently reported formula (where MT is medial thickness, VA is vessel luminal area, and MA is medial area) [3]:

$$MT\ (\mu m) = [(VA+MA)/\pi]^{1/2} - (VA/\pi)^{1/2}$$

Medial area was defined as the area from the tunica intima to the outer limit of the tunica media. The morphometric investigations of the coronary arteries were performed in vessels that had a vascular diameter ranging from 20 µm to 350 µm [3]. Interstitial and perivascular collagen volume fractions and morphometric parameters of intramyocardial coronary arteries were analyzed in the different tissue areas of each section of all five slices and averaged in each group.

For measurement of myocardial infarct size (IS), endocardial and epicardial circumferences of the whole left ventricle and of the scar tissue and the borderline between the infarcted area and the remaining myocardial muscle were marked exactly with a pointer. IS was calculated by the computer program as the percentage of the LV circumference according to the formula below:
All morphometrical measurements were performed in a blinded fashion by a single observer.

$$IS(\%) = \left[\left(\frac{\text{epicardial infarct length}}{\text{total epicardial circumference}} + \frac{\text{endocardial infarct length}}{\text{total endocardial circumference}}\right) \times \frac{1}{2}\right] \times 100.$$

### Drugs

Mibefradil was kindly provided by Hoffmann-La Roche (Grenzach-Wyhlen, Germany). The drug was given daily at a dose of 10 mg/kg per day p.o., adjusted to the individual BW of each rat. Mibefradil was dissolved in water at a concentration of 10 mg/ml. After induction of MI, food and water intake was reduced in all animals, followed by a decrease of BW. Seven days after MI the food and water intake was normalized and was no longer any different from that in sham-operated animals. During the following weeks of the experiment, no differences in food and water intake or in BW were observed among the five groups. In preliminary experiments, the dose of 10 mg mibefradil/kg per day administered daily via gastric gavage starting 7 days before the induction of MI did not significantly influence MAP or HR in infarcted animals. In these experiments, MAP and HR were measured before the induction of MI and during the following 48-h time interval after operation via a chronically implanted femoral artery catheter beginning immediately after the last p.o. administration of mibefradil (5–15 mg/kg per day) to determine a dose that does not affect cardiac function under control conditions.

### Statistical analysis

Statistical evaluation of the hemodynamic and morphometric data obtained was performed using one-way analysis of variance with repeated measures (ANOVA). Means shown to be different between individual groups were compared using the post-hoc Student's *t*-test, and differences were considered significant at $P<0.05$. Data were expressed as mean ± standard error of the mean (SEM).

## Results

### Morphometry

Cardiac weight 6 weeks after MI was examined by determining the ratio of total heart weight (THW) to body weight (BW). THW/BW was higher in groups 2 and 5 than in the sham-operated group. Cardiac weights of the animals in groups 3 and 4 tended to be lower than in group 2, but this difference was not statistically significant (Table 1).

Interstitial collagen volume fraction (ICVF), determined as a percentage of the ventricular area, was determined as a measure of interstitial fibrosis in the right

**Table 1** Morphometric data of rat hearts 6 weeks after myocardial infarction or sham surgery. Animals underwent sham surgery (*sham*), placebo treatment for MI or mibefradil treatment for MI (10 mg/kg per day) beginning 7 days before, 24 h after or 7 days after induction of MI. Data are presented as mean±SEM: Total heart weight/body weight (*THW*/*BW*), interstitial collagen volume fraction (*ICVF*) of RV, inner vascular diameter (*IVD*) of RV and LV and vascular perimeter (*VP*) of RV and LV, myocardial infarct size (*IS*)

| | Sham-operated ($n$=15) | Placebo-treated MI ($n$=15) | Mibefradil treatment for MI, starting | | |
|---|---|---|---|---|---|
| | | | 7 days before MI ($n$=13) | 24 h after MI ($n$=14) | 7 days after MI ($n$=13) |
| THW/BW | 0.310±0.01 | 0.370±0.02# | 0.330±0.01 | 0.340±0.01 | 0.360±0.02# |
| ICVF of RV (%) | 3.594±0.26 | 8.221±0.39# | 6.011±0.37*# | 7.421±0.31# | 7.998±0.30# |
| IVD of RV (mm) | 0.140±0.006 | 0.146±0.005 | 0.170±0.005*# | 0.163±0.006# | 0.159±0.006 |
| IVD of LV (mm) | 0.129±0.005 | 0.132±0.004 | 0.165±0.004*# | 0.153±0.003# | 0.149±0.006 |
| VP of RV (mm) | 0.449±0.02 | 0.467±0.02 | 0.548±0.02*# | 0.525±0.02# | 0.511±0.03 |
| VP of LV (mm) | 0.415±0.02 | 0.424±0.01 | 0.529±0.02*# | 0.492±0.02# | 0.479±0.0.03# |
| IS (%) | | 39.95±2.22 | 26.33±2.37* | 30.76±2.92 | 35.17±2.87 |

* Significant difference from placebo-treated MI ($P<0.05$); # significant difference from sham ($P<0.05$)

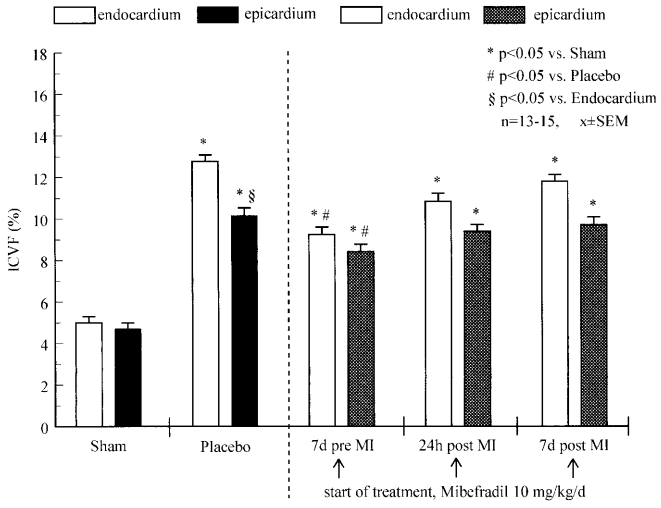


**Fig. 2** Interstitial collagen volume fraction (*ICVF*) of septal epicardium and LV endocardium as percentages 6 weeks after induction of myocardial infarction (*MI*). Animals were subjected to sham surgery, or to induction of MI and placebo treatment or mibefradil treatment (10 mg/kg per day p.o.) started at different time points before and after induction of MI (7 days before, 24 h after, 7 days after). *White columns* show ICVF of septal endocardium and *black* and *hatched columns*, ICVF of septal epicardium. Data are mean±SEM, *n*=13–15 [* significant versus sham ($P$<0.05); # significant versus placebo ($P$<0.05); § significant versus endocardium ($P$<0.05)]

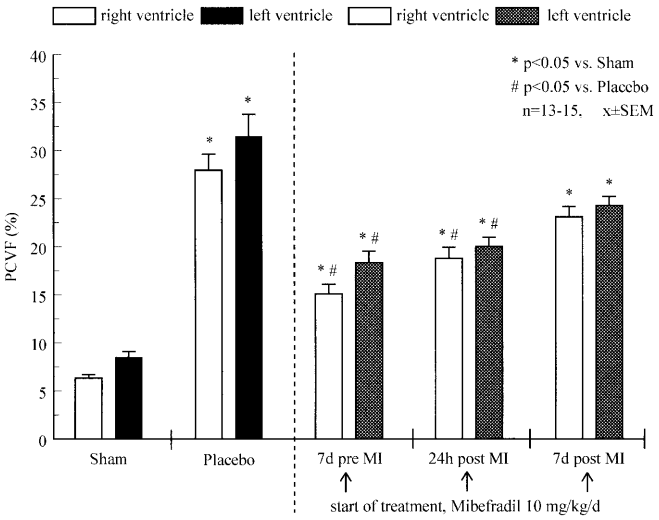


**Fig. 3** Perivascular collagen volume fraction (*PCVF*) of coronary arteries of LV and RV as percentages 6 weeks after induction of MI. Animals were subjected to sham surgery, or induction of MI and placebo treatment or mibefradil treatment (10 mg/kg per day p.o.) started at different time points before and after induction of MI (7 days before, 24 h after, 7 days after). *White columns* show ICVF of septal endocardium and *black* and *hatched columns*, that of septal epicardium. Data represent mean±SEM, *n*=13–15 [* significant versus sham ($P$<0.05), # significant versus placebo ($P$<0.05)]

ventricle, septal epicardium and septal LV endocardium. Six weeks after induction of MI, ICVF was higher in the right ventricle (Table 1) and in the septal epicardium and LV endocardium (Fig. 2) in group 2 than in the sham-operated group. LV endocardial ICVF of the placebo-treated MI group was significantly higher than epicardial ICVF. Mibefradil-treated MI groups had lower ICVF in the right ventricle when treatment was begun 7 days before MI (Table 1) and lowerseptal epicardial and LV endocardial ICVF when treatment was started 7 days before induction of MI (Fig. 2) than was observed in the placebo-treated MI group. The interstitial fibrosis in mibefradil-treated MI groups was more pronounced in the endocardial septum of the left ventricle than in the epicardial septum, but there were no significant differences. ICVF of the right ventricle was lower than ICVF of septal LV endocardium in all infarcted groups.

Perivascular collagen volume fraction (PCVF) normalized to vessel luminal area was used to determine the perivascular fibrosis of the coronary arteries. PCVF was increased in all infarcted animals (placebo-treated and mibefradil-treated) in vessels of both ventricles compared with vessels of sham-operated rats (Fig. 3). Mibefradil-treated MI rats, except for the group in which mibefradil treatment was started 7 days after MI (group 5), showed a significant reduction of coronary PCVF of both ventricles compared with arteries of placebo-treated MI rats (Fig. 3). The computerized images of picrosirius red-stained perivascular collagen areas of left ventricular coronary arteries of placebo-treated animals and group 3 animals are shown in Fig. 4A and B.

Vascular perimeter (VP), inner vascular diameter (IVD) and media thickness (MT) of the intramyocardial coronary arteries were investigated to determine the influence of post-infarct remodeling on coronary arterial morphology and to establish the degree of perivascular fibrosis. VP of intramyocardial coronary arteries of placebo-treated MI rats were not significantly different from VP of coronaries of sham-operated rats in both ventricles (Table 1). In contrast, VP of the right ventricular vessels was increased in mibefradil-treated MI rats when treatment was started 7 days before or 24 h after MI, and VP of left ventricular vessels was higher in all mibefradil-treated MI groups (Table 1) than in the sham-operated group. Compared with the placebo-treated MI group, VP of coronary arteries was higher in both ventricles in MI animals treated with mibefradil from 7 days before MI (Table 1).

IVD of intramyocardial coronary arteries of both ventricles of placebo-treated MI rats was not significantly different from that in sham-operated rats (Table 1), whereas IVD of vessels of the right ventricle was higher in mibefradil-treated MI rats when treatment was begun 7 days before or 24 h after MI than it was in sham-operated rats. IVD of left ventricular vessels was higher than in the sham-operated group in all mibefradil-treated MI groups except the group in which mibefradil treatment was started 7 days after MI (Table 1). Compared with placebo-treated MI rats, IVD of coronary arteries of both ventricles was higher in mibefradil-treated MI rats when treatment was begun 7 days prior to induction of MI (Table 1).

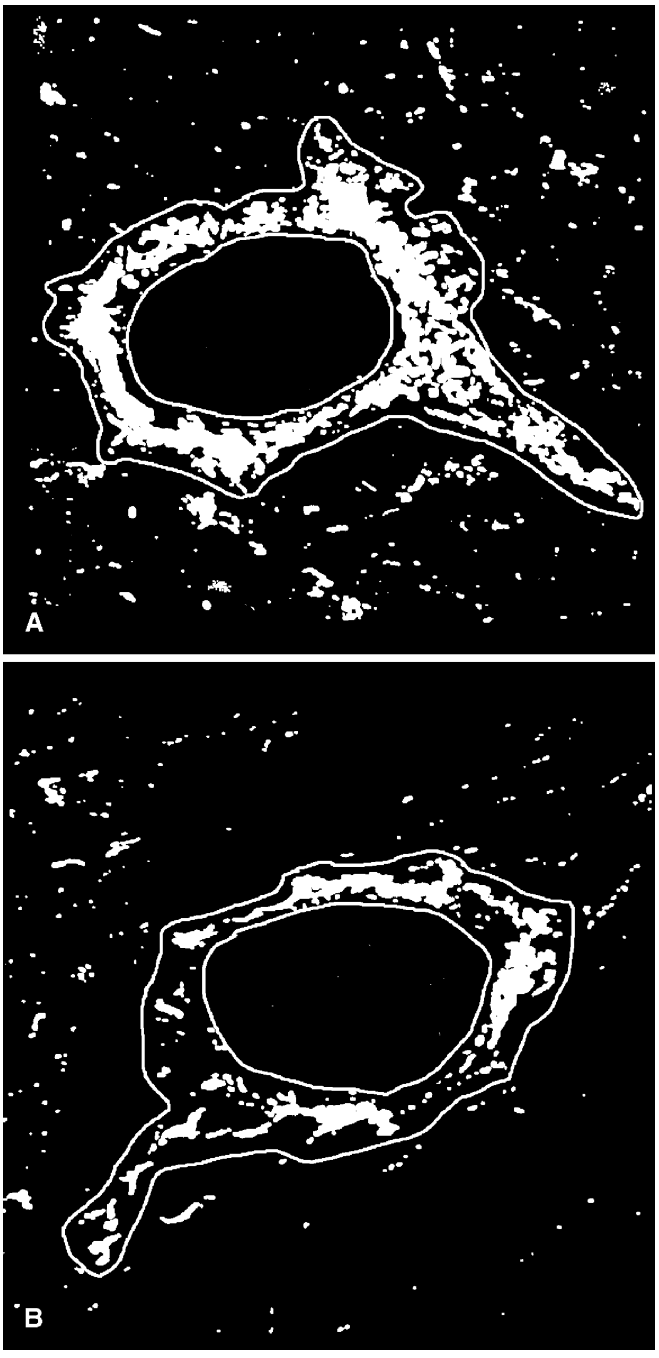


**Fig. 4A, B** Representation of computerized images of picrosirius red-stained perivascular collagen areas of left ventricular coronary arteries of **A** placebo-treated and **B** mibefradil-treated MI animals (treated 7 days before MI) 6 weeks after induction of MI. Mibefradil-pretreated MI animals show a less perivascular collagen of coronary arteries of LV than do placebo-treated MI animals

MT of coronary arteries was higher in placebo-treated MI animals than in sham-operated animals (Fig. 5). Animals in group 3 and group 4 showed a significantly smaller MT than placebo-treated MI animals. MT of vessels of both ventricles was not significantly larger in group 3 animals than in sham-operated animals (Fig. 5).

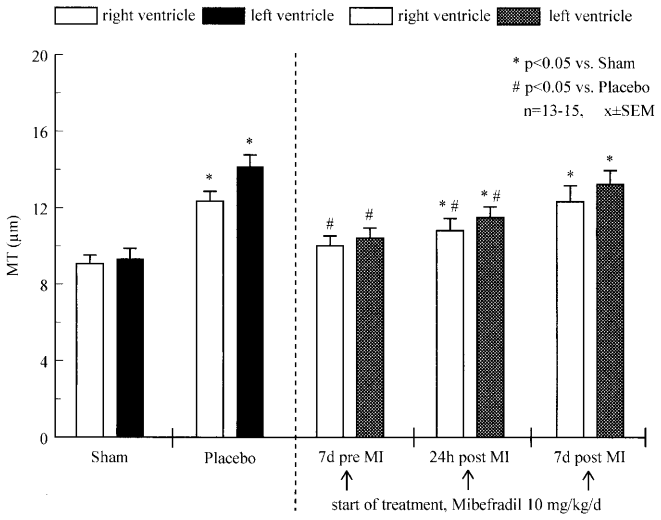


**Fig. 5** Media thickness (*MT*) of coronary arteries of RV and LV in micrometers 6 weeks after induction of MI. Animals were subjected to sham surgery, placebo treatment or mibefradil treatment (10 mg/kg per day p.o.) started at different time points before and after induction of MI (7 days before, 24 h after, 7 days after). *White columns* show MT of coronary arteries of RV and *black* and *hatched columns*, MT of coronary arteries of LV. Data are mean±SEM, $n$=13–15 [* significant versus sham ($P$<0.05), # significant versus placebo ($P$<0.05)]

Myocardial infarct size (IS), determined as the percentage of the LV circumference, was 39±2% in the placebo-treated MI group (Table 1). Chronic mibefradil treatment started 7 days prior to induction of MI was followed by lower IS values than in placebo-treated MI rats. No significantly smaller IS was observed when mibefradil treatment was started 24 h or 7 days after coronary ligation (Table 1).

## Hemodynamics

Mean arterial blood pressure (MAP), measured in preliminary experiments in separate groups ($n$=6–8) during surgery and during the 48-h time interval after operation, was lower in group 2 and in group 3 immediately after MI and during the following 48-h period than in sham-operated animals. No significant differences were seen between the placebo-treated MI group and the mibefradil-treated group (Fig. 6). Heart rate (HR) was higher in groups 2 and 3 than in the sham-operated group. Animals in group 3 showed a tendency to have lower HR than those in the placebo-treated MI group (data not shown).

At the end of the experiment, 6 weeks after induction of MI peripheral (MAP, HR) and left ventricular ($dP/dt_{max}$, LVEDP), hemodynamic parameters were measured to determine the cardiac function. At this time point, a decrease in MAP and $dP/dt_{max}$ and an increase in LVEDP at baseline and after methoxamine stimulation were observed in placebo-treated MI animals compared with sham-operated animals (Figs. 7–9). To test cardiac

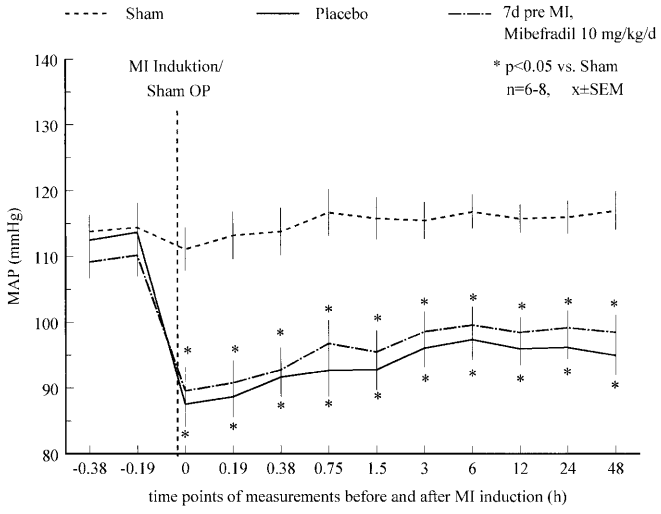


**Fig. 6** Mean arterial blood pressure (*MAP*) during surgery and during the 48-h time interval after operation. Animals were subjected to sham surgery (*sham*), placebo (s) and mibefradil treatment (10 mg/kg per day p.o.) beginning 7 days before induction of MI *(7 days pre*). Data are mean±SEM, *n*=6–8 [* significant versus sham (*P*<0.05)]

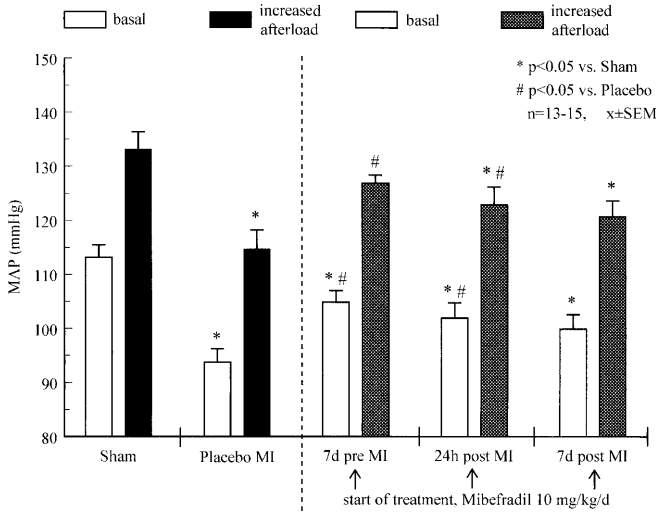


**Fig. 7** Mean arterial blood pressure (MAP) at baseline and after increased afterload 6 weeks after induction of MI. Animals were subjected to sham surgery or to MI induction and placebo treatment or mibefradil treatment (10 mg/kg per day p.o.) started at different time points before and after induction of MI (7 days before, 24 h after, 7 days after). *White columns* show MAP at baseline and *black* and *hatched columns*, MAP after increased afterload. Data are mean±SEM, *n*=13–15 [* significant versus sham (*P*<0.05), # significant versus placebo (*P*<0.05)]

function after increased afterload, methoxamine infusion was initiated and steadily increased until MAP was 20 mmHg higher than baseline in all groups. Animals in group 2 needed higher doses of methoxamine to increase blood pressure by 20 mmHg than did the sham-operated animals. In contrast, the consumption of methoxamine needed to increase blood pressure by 20 mmHg was lower in mibefradil-treated MI animals when treatment was begun 7 days before MI (data not shown).

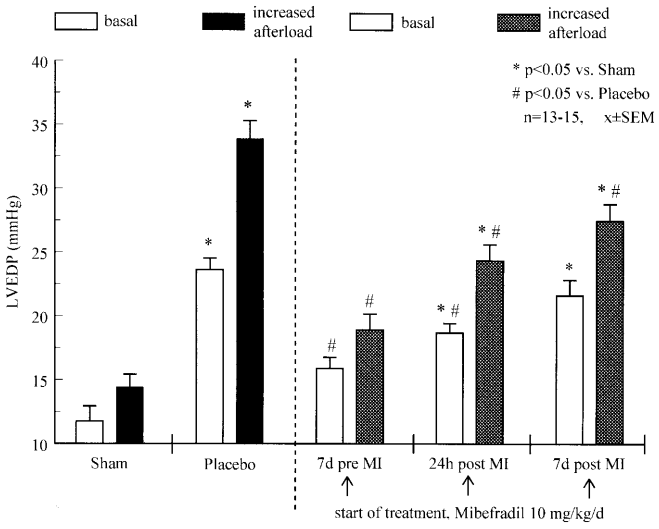


**Fig. 8** Left ventricular end-diastolic pressure (*LVEDP*) at baseline and after increased afterload 6 weeks after induction of myocardial infarction (*MI*). Animals subjected to sham surgery, placebo-treated MI rats and mibefradil-treated MI animals (10 mg/kg per day p.o.) with mifebradil treatment started at different time points before and after induction of MI (7 days before, 24 h after, 7 days after). *White columns* show LVEDP at baseline and *black* and *hatched columns*, after increased afterload. Data represent mean ±SEM, n=13–15 [* significant versus sham (*P*<0.05), # significant versus placebo (*P*<0.05)]

Six weeks after the induction of MI, MAP was decreased in all infarcted rats compared with the sham-operated animals. In contrast, mibefradil-treated animals in groups 3 and 4 showed higher MAP values at baseline and after increased afterload than the placebo-treated MI group. MAP of 7 rats in group 3 differed insignificantly from that in sham-operated rats after methoxamine stimulation (Fig. 7).

HR at week 6 after MI/sham surgery did not differ significantly between the sham-operated and placebo-treated MI rats at baseline or after methoxamine infusion. HR tended to be lower in all mibefradil-treated MI animals than in the placebo-treated MI group, but this difference was not statistically significant (data not shown).

Placebo-treated MI rats had higher LVEDPs at baseline and during increased afterload than those that underwent sham surgery. In two of the mibefradil-treated MI groups (groups 2 and 3), LVEDP at baseline was lower than in the placebo-treated MI group. LVEDP of all mibefradil-treated groups was reduced after methoxamine stimulation. LVEDP of mibefradil-treated animals was higher in groups 4 and 5 at baseline and after methoxamine stimulation than in the sham-operated group. In contrast to the other mibefradil-treated MI groups, LVEDP in group 3 was not significantly higher at baseline and after methoxamine stimulation than it was in the sham-operated group (Fig. 8).

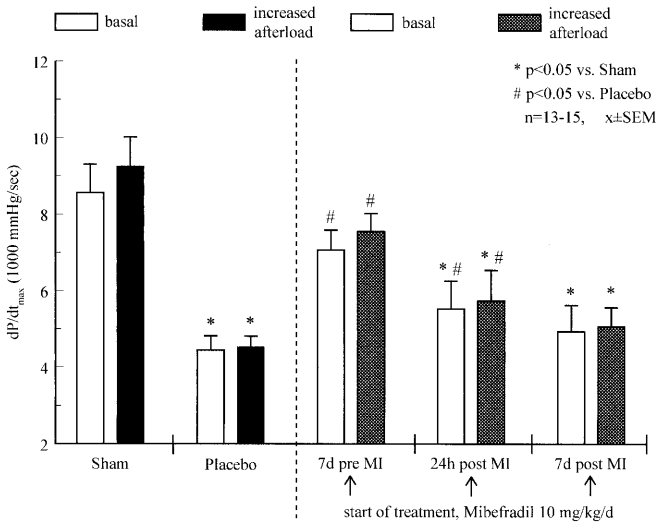


**Fig. 9** Cardiac contractility ($dP/dt_{max}$) at baseline and after increased afterload 6 weeks after induction of MI. Animals subjected to sham surgery, placebo-treated MI animals and mibefradil-treated MI animals (10 mg/kg per day p.o.) started at different time points before and after induction of MI (7 days before, 24 h after, 7 days after). *White columns* show $dP/dt_{max}$ at baseline and *black* and *hatched columns*, after increased afterload. Data represent mean±SEM, $n$=13–15 [* significant versus sham ($P$<0.05), # significant versus placebo ($P$<0.05)]

$dP/dt_{max}$ at baseline and during increased afterload was lower in placebo-treated MI rats than in sham-operated animals. $dP/dt_{max}$ was higher at baseline and after methoxamine stimulation in group 3 than in placebo-treated MI rats. In this group cardiac contractility did not differ from the sham-operated group at baseline or after methoxamine stimulation. $dP/dt_{max}$ was lower in groups 4 and 5 at baseline and after methoxamine stimulation than in sham-operated animals (Fig. 9).

## Discussion

The purpose of the present investigation was to examine the effects of the mixed L- and T-type CCA, mibefradil, on structural remodeling of cardiac interstitium and coronary vasculature and on ventricular performance in MI-induced cardiac failure.

The experimental model used features pronounced heart disease associated with impaired cardiac function 6 weeks after coronary ligation. At this point, the remodeling process has usually taken place and stable hemodynamic conditions can be expected [4]. In our study, placebo-treated MI rats showed a higher left ventricular end-diastolic pressure (LVEDP) and a lower cardiac contractility ($dP/dt_{max}$) accompanied by an impaired peripheral blood flow evidenced by a reduction in mean arterial blood pressure (MAP). Additionally, animals in the placebo-treated MI group had a higher ratio of THW to BW, associated with an increased interstitial collagen content in the right ventricle and in the septal epicardium and LV endocardium. These cardiac alterations were accompanied by an elevated perivascular collagen content of the intramyocardial coronary arteries of both ventricles, indicating that the infarct had induced cardiac hypertrophy and engendered myocardial and perivascular fibrosis. Our data are in agreement with the results of several studies demonstrating that the development of myocardial fibrosis is related to hypertrophy induced by either hypertension or heart failure and is accompanied by the predominant accumulation of collagen type I and III within the interstitial space and the adventitia of intramyocardial coronary arteries [7, 49]. Continued structural remodeling leads to increased myocardial stiffness, accounting in part for the progressive deterioration in the mechanical behavior of the myocardium [15, 17]. The fact that the interstitial collagen content of the LV endocardium was more markedly increased than that of the epicardium has been interpreted as an indication that the structural remodeling of the inner left ventricular wall seems to be related to the increased wall stress, which depends on the degree of left ventricular pressure overload [44].

The increased accumulation of perivascular collagen around the coronary arteries of placebo-treated MI animals was associated with an increase in media thickness (MT), but without changes of vascular perimeter (VP) or inner diameter (IVD). Whereas the lumen of the vessels remained constant the MT was elevated, suggesting an increase in the amount of wall material including growth and/or proliferation of medial smooth muscle cells. According to the different patterns of vascular remodeling described by Mulvany et al. [34], placebo-treated MI animals showed hypertrophic noninward vascular remodeling associated with limited vasomotor reactivity and impaired coronary flow reserve leading to worsened myocardial perfusion.

In contrast to the situation in placebo-treated MI animals, LVEDP under basal conditions was reduced in groups 3 and 4 and in all mibefradil-treated MI animals (groups 3–5) during increased afterload. Additionally, CCA-pretreated MI animals showed higher $dP/dt_{max}$ at baseline and after methoxamine stimulation. Indeed, LVEDP and $dP/dt_{max}$ of animals in group 3 were not significantly different from those of sham-operated animals. These findings indicate an improved myocardial performance evidenced by an increase in peripheral blood pressure. In groups 3 and 4 heart weight was no higher than that in sham-operated animals, indicating the overall advantageous effect of early calcium channel blocker therapy. In addition, mibefradil-pretreated MI rats showed a reduction in the interstitial and perivascular collagen content of the right ventricle and of the septal epicardium and LV endocardium, suggesting that early treatment with mibefradil attenuated the reactive fibrosis of the myocardial interstitium. Furthermore, the perivascular fibrosis was also prevented when mibefradil treatment was initiated up to 7 days after MI. Hence, the prevention of cardiac remodeling seems to be a drug-related effect demonstrated by more effective attenuation of perivascular fibrosis than of interstitial fibrosis. This

finding is compatible with an earlier report demonstrating more effective prevention of perivascular than of interstitial cardiac fibrosis after 6 weeks of treatment with mibefradil in two-kidney/one-clip renovascular hypertensive rats [53].

Since reactive fibrosis is not related to myocyte necrosis and is independent of the size of myocardial infarct [6, 48] the ability of CCA to decrease interstitial collagen content seems to be directly or indirectly related to modulation of collagen synthesis and/or degradation via influence of $Ca^{2+}$-dependent intracellular signaling mechanisms in cardiac fibroblasts [39]. Several studies have indicated that CCA block the $Ca^{2+}$ entry by way of voltage-sensitive L-type calcium channels into fibroblasts [39, 47], and that this is associated with a reduction in collagen synthesis and an inhibition of attachment and proliferation of human fibroblasts [25]. Additionally, an increased left ventricular pressure has also been considered to be responsible for a rise in cytosolic $Ca^{2+}$ that activates collagen synthesis in cardiac fibroblasts [35]. Thus, in combination with the reduction of LVEDP, CCA obviously attenuate the detrimental increase of intracellular $Ca^{2+}$ in fibroblasts, resulting in a decreased collagen synthesis and, consequently, in prevention of myocardial fibrosis and cardiac hypertrophy.

The capacity of CCA to modulate the effects of such mitogenic factors as endothelin [31, 36] or aldosterone [27, 29] in fibroblasts has also been demonstrated. In these experiments nifedipine attenuated the rise in intracellular $Ca^{2+}$ induced by increased plasma endothelin during hypertension or heart disease. This effect of nifedipine was associated with a reduced protein kinase C (PKC) activity and phosphoinositol metabolism, which resulted in a reduced production of cellular proteins and decreased collagen synthesis in dermal fibroblasts [24, 36]. Mibefradil has also been demonstrated to reduce the endothelin-induced activation of PKC in isolated smooth muscle cells [19], indicating that mibefradil exerts antifibrotic effects on the arterial vasculature. Additionally, CCA of the dihydropyridine type blocked potassium- and angiotensin II-induced release of aldosterone from adrenal glomerulosa cells [27, 29] and, thus, indirectly affected collagen synthesis and degradation via modulation of the renin-angiotensin-aldosterone system. The fact that the angiotensin II-induced release of aldosterone and renin is regulated by a T-type calcium channel-related mechanism [8, 13] indicates that the blockade of this channel type by mibefradil reduced the release of these hormones.

The greater efficacy of mibefradil to prevent perivascular fibrosis than interstitial fibrosis could be related to the selectivity of the drug for the coronary vasculature [41, 42]. Mibefradil has been shown to induce a dilatation of coronary arteries, as evidenced by increased myocardial coronary blood flow [26, 53] and by our morphometric data (Table 1). Generally, an increase of coronary reserve has been attributed to the decrease in the thickness of the vessel wall and to the improvement of vascular performance of coronary arteries and/or to the reduction of perivascular fibrosis [10].

In addition, evidence has been presented that T-type calcium channels participate in the regulation of growth and proliferation of vascular smooth muscle cells [16, 45], and the activity and expression of this channel type are increased in failing hearts [5, 38], suggesting an influence of this channel type on the regulation of intracellular $Ca^{2+}$ levels in pathologic conditions. Thus, the prevention of perivascular fibrosis and the reduction of MT by mibefradil seems to be related in part to the T-type calcium channel-blocking action of the drug [30].

In our experiments, mibefradil-treated MI rats showed higher VP and IVD of the coronary arteries than sham-operated animals. These vascular alterations were accompanied by a smaller MT, which was significantly different from that in placebo-treated MI rats when mibefradil treatment was started 7 days before or 24 h after MI. Thus, chronic mibefradil treatment induced an increase in the patent diameter of the vascular lumen and prevented an increase in the amount of vascular material of coronary arteries in infarcted rat hearts. These structural alterations to the arteries have been termed hypotrophic outward remodeling [33]. The reduction of media hypertrophy in combination with the marked vasodilation by mibefradil in spite of adventitial fibrosis could be explained in part by the prevention of angiotensin II- and/or endothelin-induced smooth muscle cell proliferation and/or vasoconstriction [26].

In summary, chronic mibefradil treatment improved cardiac performance and effectively prevented the development of reactive and perivascular fibrosis evidenced by decreased collagen accumulation in the interstitial space and around coronary arteries in failing hearts after MI. The compound exerted an antifibrotic and cardioprotective action via limitation of vascular remodeling and improved vascular performance of coronary arteries, thereby increasing myocardial perfusion. A contribution of T-type calcium channels in remodeling processes in heart failure and the property of mibefradil to block T-type and L-type calcium channels seems to give the drug the potential for a positive influence on the pathologic changes in the myocardium that are associated with congestive heart failure, which has not been demonstrated for pure L-type CCA [18].

**Acknowledgements** The authors thank Dr. R. Schulz and Professor D. Harms (Department of Pediatric Pathology, Christian-Albrechts-University Kiel, Germany) for their kind support with the histological procedures.

## References

1. Anversa P, Loud AV, Levicky V, Guideri G (1985) Left ventricular failure induced by myocardial infarction.I. Myocyte hypertrophy. Am J Physiol 248:H876-H882
2. Anversa P, Beghi C, Kikkawa Y, Olivetti G (1986) Myocardial infarction in rats: infarct size, myocyte hypertrophy and capillary growth. Circ Res 58:26–37
3. Atherton GW, Cabric M, James NT (1982) Stereological analysis of capillaries in muscle of dystrophic mice. Virchows Arch 397:347–354

4. Ball SG (1995) Myocardial infarction – from trials to practice. Wrightson Biomedical, Petersfield UK Bristol Pa, pp 25–46
5. Bogdanov KY, Ziman BD, Spurgeon HA, Lakatta EG (1995) L- and T-type calcium currents differ in finch and rat ventricular cardiomyocytes. Mol Cell Cardiol 27:2581–2593
6. Brilla C, Janicki JS, Weber KT (1991) Impaired diastolic function and coronary reserve in genetic hypertension: role of interstitial fibrosis and medial thickening of intramyocardial coronary arteries. Circ Res 69:107–115
7. Brilla CG, Pick R, Tan LP, Janicki JS, Weber KT (1990) Remodeling of the rat right and left ventricles in experimental hypertension. Circ Res 67:1355–1364
8. Buisson B, Laflamme L, Bottari S, et al (1995) A G protein is involved in the angiotensin $AT_2$ receptor inhibition of the T-type calcium current in non-differentiated NG108–15 cells. J Biol Chem 270:1670–1674
9. Burton AC (1954) Relation of structure to function of the tissue of the wall of blood vessels. Physiol Rev 34:619–642
10. Canby CA, Tomanek RJ (1989) Role of lowering arterial pressure on maximal coronary flow with and without regression of cardiac hypertrophy. Am J Physiol 257:H1110–H1118
11. Clozel JP, Banken L, Osterrieder W (1989) Effects of RO 40-5967, a novel calcium antagonist, on myocardial function during ischemia induced by lowering coronary perfusions pressure in dogs: comparison with verapamil. J Cardiovasc Pharmacol 14:713–721
12. Contard F, Koteliansky V, Marotte F, Dubud I, Rappaport L, Samuel JL (1991) Specific alterations in the distribution of extracellular matrix components within rat myocardium during the development of pressure overload. Lab Invest 64:65–75
13. DeGasparo M, Bottari S, Levens N (1995) Characteristics of angiotensin II receptors and their role in cell and organ physiology. In: Laragh J, Brenner B (eds) (1995) Hypertension: pathology, diagnosis, and management, 2nd edn. Raven Press, New York, pp 1695–1720
14. Doering CW, Jalil JE, Janicki JS, Pick R, Aghili S, Abrahams C, Weber KT (1988) Collagen network remodeling and diastolic stiffness of rat left ventricle with pressure overload hypertrophy. Cardiovasc Res 22:686–695
15. Gay RG (1990) Early and late effects of captopril treatment after large myocardial infarction in rats. JACC 16:967–977
16. Gray G, Clozel M, Clozel JP, Baumgartner HR (1993) Effects of calcium channel blockade on the aortic intima in spontaneously hypertensive rats. Hypertension 22:569–576
17. Hartmann JC, Hullinger TG, Wall TM, Shebusky RJ (1993) Reduction of myocardial infarct size by ramiprilat is independent of angiotensin II synthesis inhibition. Eur J Pharmacol 234:229–236
18. Held PH, Yusuf S, Furberg CD (1989) Calcium channel blockers in acute myocardial infarction and unstable angina: an overview. BMJ 299:1187–1192
19. Hermsmeyer K, Miyagawa K (1996) Protein kinase C mechanism enhances vascular muscle relaxation by the $Ca^{2+}$ antagonist, RO 40-5967. J Vasc Res 33:71–77
20. Isoyama S, Ito N, Satoh K, Takishima T (1992) Collagen deposition and the reversal of coronary reserve in cardiac hypertrophy. Hypertension 20:491–500
21. Jalil JE, Janicki JS, Pick R, Shroff SG, Weber KT (1989) Fibrillar collagen and myocardial stiffness in the intact hypertrophied rat left ventricle. Circ Res 64:1041–1050
22. Jugdutt BI, Amy RWM (1986) Healing after myocardial infarction in the dog: changes in infarct hydroxyproline and topography. J Am Coll Cardiol 7:91–102
23. Junqueira LC, Bignolas G, Brentani RR (1979) Red sirius staining plus polarizing microscopy: a specific method for collagen detection in tissue sections. Histochem J 79:445–447
24. Kahaleh MB (1991) Endothelin, an endothelial-dependent vasoconstrictor in scleroderma. Enhanced production and profibrotic action. Arthritis Rheum 34:978–983
25. Kang Y, Lee DA, Higginbotham EJ (1997) In vitro evaluation of antiproliferative potential of calcium channel blockers in human Tenon's fibroblasts. Exp Eye Res 64:913–925
26. Karam H, Heudes D, Bruneval P, Gonzales MF, Löffler BM, Clozel M, Clozel JP (1996) Endothelin antagonism in end-organ damage of spontaneously hypertensive rats. Comparison with angiotensin-converting enzyme inhibition and calcium antagonism. Hypertension 28:379–385
27. Kojima K, Kojima I, Rasmussen H (1984) Dihydropyridine calcium agonist and antagonist effects on aldosterone secretion. Am J Physiol 247:E645–E650
28. Medugorac I, Jacob R (1983) Characterization of left ventricular collagen in the rat. Cardiovasc Res 17:15–21
29. Millar JA, McLean KA, Sumner DJ, Reid JL (1983) The effect of the calcium antagonist on pressor and aldosterone responses to angiotensin II in normal man. Eur J Clin Pharmacol 24: 315–321
30. Mishra SK, Hermsmeyer K (1994) Selective inhibition of T-type calcium channels by RO 40-5967. Circ Res 75:144–148
31. Miyauchi T, Ishikawa T, Tomobe Y, et al (1989) Characteristics of pressure response to endothelin in spontaneously hypertensive and Wistar-Kyoto rats. Hypertension 14:427–434
32. Morkin E. Ashford TP (1968) Myocardial DNA synthesis in experimental cardiac hypertrophy. Am J Physiol 215:1409–1413
33. Mulvany MJ, Hansen PK, Alkjaer C (1978) Direct evidence that the greater contractility of resistance vessels in spontaneously hypertensive rats is associated with a narrowed lumen, a thickened media and an increased number of smooth muscle cell layers. Circ Res 43:854–864
34. Mulvany MJ, Baumbach GL, Aalkjaer C, Heagerty AM, Korsgaard N, Schiffrin EL, et al (1996) Vascular remodeling. Hypertension 28:505–506
35. Nayler WG, Britnell S (1991) Calcium antagonists and tissue protection. J Cardiovasc Pharmacol 18(1):S1-S5
36. Nayler WG, Liu J, Panagiotopoulos S (1990) Nifedipine and experimental cardioprotection. Cardiovasc Drugs Ther 4:879–886
37. Nicoletti A, Heudes D, Hinglais N, Appay MD, Philippe M, Sassy-Prigent C, Bariety J, Michel JB (1995) Left ventricular fibrosis in renovascular hypertensive rats. Effects of losartan and spironolactone. Hypertension 26:101–111
38. Nuss BH, Houser SR (1993) T-type calcium current is expressed in hypertrophied adult feline left ventricular myocytes. Circ Res 73:777–782
39. Olsen R, Seewald M, Powis G (1989) Contribution of external and internal $Ca^{2+}$ to changes in intracellular free $Ca^{2+}$ produced by mitogens in Swiss 3T3 fibroblasts: the role of dihydropyridine sensitive $Ca^{2+}$ channels. Biochem Biophys Res Commun 162:448–455
40. Opie LH (ed) (1984) Calcium antagonists and cardiovascular disease. Raven Press, New York, pp 1–377
41. Orito K, Satoh K, Taira N (1993) Cardiovascular profile RO 40-5967, a new nondihydropyridine calcium channel antagonist, delineated in isolated, blood perfused dog hearts. J Cardiovasc Pharmacol 22:293–299
42. Osterrieder W, Holck M (1989) In vitro pharmacologic profile of RO 40–5967, a novel calcium channel blocker with potent vasodilatator but weak inotropic action. J Cardiovasc Pharmacol 13:754–759
43. Pfeffer MA, Braunwald E (1990) Ventricular remodeling after myocardial infarction. Circulation 81:1161–1172
44. Pfeffer MA, Pfeffer JM, Fishbein MC, Fletcher PJ, Spadaro J, Kloner RA, Braunwald E (1979) Myocardial infarct size and ventricular function in rats. Circ Res 44:503–512
45. Richard S, Neveu D, Carnac G, Bodin P, Travo B, Nargeot J (1992) Differential expression of voltage-gated $Ca^{2+}$ -current in cultivated aortic myocytes. Biochim Biophys Acta 1160:95–104
46. Riede U, Reith A (1980) Morphometry in pathology. (Research and practice, vol 166) Fischer, Stuttgart, pp 2–3
47. Salo T, Oikarinen KS, Oikarinen AI (1990) Effect of phenytoin and nifedipine on collagen gene expression in human gingival fibroblasts. J Oral Pathol Med 19:404–407
48. Sawamura I, Hazama F, Kinoshita M (1990) Histological and histometrical study of myocardial fibrosis in spontaneously hypertensive rats of the stroke-prone strain. Jpn Circ J 54: 1274–1282

49. Sen S, Bumpus M (1979) Collagen synthesis in development and reversal of cardiac hypertrophy in spontaneously hypertensive rats. Am J Cardiol 44:954–958
50. Stauss B, Itoi K, Stauss H, Unger T (1990) A novel inexpensive computer system to record and analyze hemodynamic data in conscious animals. Eur J Pharmacol 183:863–864
51. Stauss HM, Zhu Y-C, Redlich TH, Adamiak D, Mott, Kregel KC, Unger T (1994) Angiotensin-converting enzyme inhibition in infarct-induced heart failure in rats: bradykinin versus angiotensin II. J Cardiovasc Risk 1:255–262
52. Veniant M, Clozel JP, Hess P, Wolfgang R (1991) RO 40-5967, in contrast to diltiazem, does not reduce left ventricular contractility in rats with chronic myocardial infarction. J Cardiovasc Pharmacol 17:277–284
53. Veniant M, Clozel JP, Heudes D, Banken L, Menard J (1993) Effects of RO 40-5967, a new calcium antagonist, and enalapril on cardiac remodeling in renal hypertensive rats. J Cardiovasc Pharmacol 21:544–551
54. Weber KT, Brilla C, Janicki JS (1990) Structural remodeling of myocardial collagen in systemic hypertension: functional consequences and potential therapy. Heart Failure 6:129–137
55. Weber KT, Janicki JS, Shroff SG, Pick R, Chen RM, Bashey RI (1988) Collagen remodeling of the pressure-overloaded, hypertrophied nonhuman primate myocardium. Circ Res 62:757–765
56. Wicker P, Tarazi RC, Kobayashi K (1983) Coronary blood flow during the development and regression of left ventricular hypertrophy in renovascular hypertensive rats. Am J Cardiol 51:1744–1749